Turbulence spectra from a tidal channel

By H. L. GRANT, R. W. STEWART† AND A. MOILLIET

Pacific Naval Laboratory of the Defence Research Board of Canada, Esquimalt, B.C., Canada

(Received 22 July 1961)

This paper describes the use of a hot film flowmeter in the sea and presents experimental measurements of the 'downstream' component of turbulent velocity in a tidal channel. The Reynolds number of the flow is about 10^8 and the scale of the turbulence is so large that a ship is carried about to a considerable extent by the energy-containing eddies. Under these conditions, a velocity measuring probe attached to a ship cannot be used for reliable measurements in the energy-containing range of the spectrum. It is possible, however, to observe the inertial and dissipation ranges. Records have been made at various stages of the tide. The one-dimensional spectra are found to be proportional to $k^{-\frac{5}{3}}$ for several decades in k as predicted by Kolmogoroff, and a value is given for Kolmogoroff's constant. In the dissipation range there is close agreement with both Kovasznay's theory and Heisenberg's theory. These two theories are not very different in the low wave-number end of the range and the observations do not extend to high enough wave-numbers to distinguish between them.

1. Introduction

A very large proportion of theoretical work on turbulence during the last decade or so has been concerned with the high wave-number part of the energy spectrum. The reason is clear: at lower wave-numbers, which contain almost all the turbulent energy, the structure of the turbulence is determined by the mean flow upon which it is superimposed. The turbulence, except in some very atypical situations, is highly anisotropic and the difficulties of theoretical treatment are formidable in the extreme. For the high wave-numbers, however, there is some hope that the field may be considered to be homogeneous and isotropic, with a resulting great simplification in analysis. There is also the expectation that at high enough wave-numbers the turbulence will be so de-coupled from the particular mean flow which supplies the energy that any results obtained may be said to be characteristic of turbulence as such, rather than of turbulence derived from a particular flow.

The notion that the smallest scales of turbulent motion have a behaviour independent of the details of the energy-containing scales was first put forward by Kolmogoroff (1941), and is generally referred to as 'Kolmogoroff's Hypothesis'. Komolgoroff originally presented his idea in terms of the difference in velocity of neighbouring points in the field. Current preference, however, is to

† Now at University of British Columbia, Vancouver, B.C.

carry on the discussion in terms of the wave-number k of the Fourier decomposition of the field (e.g. Batchelor 1953; Hinze 1959).

In theoretical discussions of isotropic turbulence, it is generally considered that the mathematically definable entity which has the closest correspondence to the physical notion of the energy associated with a particular scale of motion is the three-dimensional spectral density function $E(k)$ (Batchelor 1953),

$$\int_0^\infty E(k)\,dk = \tfrac{1}{2}q^2 = \tfrac{1}{2}(\overline{u}^2+\overline{v}^2+\overline{w}^2), \tag{1.1}$$

where u, v and w are turbulent velocity components.

No way is known by which $E(k)$ may be measured directly. Experimental measurements are made of the one-dimensional spectrum function $\phi(k)$, where

$$\int_0^\infty \phi(k)\,dk = \overline{u}^2, \tag{1.2}$$

which is related (Hinze 1959, p. 171) to $E(k)$ by

$$2E(k) = k^2\frac{\partial^2\phi(k)}{\partial k^2} - k\frac{\partial\phi(k)}{\partial k}. \tag{1.3}$$

It should be noted that the factor $\frac{1}{2}$ is customarily used in the definition of $E(k)$, as in (1.1) (except by Stewart & Townsend 1951), but that the definition of $\phi(k)$ is not uniform in the literature. The form (1.2) above is commonly used in experimental work and is used in the book by Hinze (1959) where the corresponding quantity is $E_1(k)$. Most theoretical works, including the book by Batchelor (1953), have used a $\phi(k)$ which is half as large as that defined above.

When concern is with the small scales of motion, the most important parameter of the turbulence is the energy-dissipation density ϵ†. It can be shown (Hinze 1959) that

$$\epsilon = 2\nu\int_0^\infty k^2E(k)\,dk = 15\nu\int_0^\infty k^2\phi(k)\,dk, \tag{1.4}$$

where ν is the kinematic viscosity.

The functions $k^2E(k)$ and $k^2\phi(k)$ are referred to as dissipation spectra, and describe the distribution in wave-number of the rate of decay of turbulent energy to heat.

In these terms Kolmogoroff's hypothesis states that at sufficiently high wave-numbers the only parameters which can affect the energy density $E(k)$ at wave-number k are the rate of energy-dissipation density ϵ and the kinematic viscosity ν.

In general it might be expected that $\partial\epsilon/\partial t$ would also be an important parameter. However, it can be shown (Corrsin 1958) that the characteristic time-scale of the turbulence decreases as k increases. Thus, for sufficiently large wave-numbers $\epsilon/(d\epsilon/dt)$ becomes large compared with the characteristic time-scale, and the turbulence may be treated as though in a steady state—the Kolmogoroff steady state.

† It is customary to use kinematic terms, where 'densities' are per unit mass. E then has dimensions L^2T^{-2} and ϵ, L^2T^{-3}.

With this assumption, dimensional arguments then lead to the conclusion

$$E(k) = \epsilon^{\frac{2}{3}} k^{-\frac{5}{3}} F(k/k_s), \tag{1.5}$$

where

$$k_s = (\epsilon/\nu^3)^{\frac{1}{4}}. \tag{1.6}$$

Kolmogoroff's hypothesis then asserts that the function $F(k/k_s)$ is a universal one, common to all fields of turbulence provided that k is sufficiently large that the motion is de-coupled from the main features of the flow.

No very satisfactory theory is available which provides a form for $F(k/k_s)$. The three best known attempts are those of Obukhov (1941), Heisenberg (1948) and Kovasznay (1948), each of which is based upon a different assumption about the nature of the transfer of energy from one part of the spectrum to another. No discussion of the merits of these, or other, theories is warranted here. The assumptions and results are compared by Hinze (1959) and by Reid (1960). It is usual to construct these theories in terms of the three-dimensional spectrum $E(k)$,† which, as noted above, is not measured. Comparison with experiments has therefore been difficult because it happens that the transformation from $E(k)$ to $\phi(k)$ is much less simple than the inverse, given in (1.3). The alternative procedure of transforming experimental values of $\phi(k)$ to $E(k)$ is not attractive because of the uncertainty which experimental error introduces into $\partial^2\phi/\partial k^2$. Reid (1960) has performed a valuable service in tabulating values of $\phi(k)$ obtained by transforming numerically the $E(k)$ spectra which result from the assumptions of Obukhov, Kovasznay and Heisenberg. Each of these theories has just one free parameter which must be determined empirically.

More important than a detailed check upon these theories is a check of the accuracy of (1.5) itself. In particular, it is well known that if the hypotheses leading to (1.5) hold for a range of wave-numbers upon which viscosity has little direct effect (the inertial subrange), then $E(k)$ must be independent of k_s, so that

$$F(k/k_s) = K, \tag{1.7}$$

where K is a constant.

It is clear from (1.3) that for any region in which $E(k)$ has power law form, $\phi(k)$ also has power law form. Thus corresponding to (1.7) will be a region where

$$\phi(k) = K' \epsilon^{\frac{2}{3}} k^{-\frac{5}{3}}, \tag{1.8}$$

where

$$K' = \tfrac{18}{55} K. \tag{1.9}$$

K' is an absolute constant provided (1.5) holds. Its evaluation is obviously very important. Although the nature of $F(k/k_s)$ is evidently of great interest, rather little is known of it experimentally. It can be shown (Stewart & Townsend 1951) that in ordinary laboratory grid-produced turbulence, the assumption of steady state is not valid except for wave-numbers so large that they contribute little even to the dissipation spectrum. Recently, Kistler & Vrebalovich (1961) have been able to conduct some grid-turbulence experiments in the very large Co-operative Wind Tunnel at Pasadena. They were able to achieve Reynolds numbers sufficiently high to obtain a form for $F(k/k_s)$. Unfortunately, it was

† Kovasznay originally formulated his in terms of $\phi(k)$, but succeeding authors have considered $E(k)$ more suitable.

necessary to dismantle this facility before the full import of some unexpected aspects of their measurements, notably high wave-number anisotropy, could be investigated.

Measurements in laboratory pipes (Laufer 1954), boundary layers (Klebanoff 1955) and channels (Laufer 1951) have not convincingly demonstrated the correctness of (1.5) or the form of $F(k/k_s)$. Apparently ordinary laboratory flows do not provide turbulence of sufficiently high Reynolds number for Kolmogoroff's hypothesis to be properly tested, although Betchov (1957) has measured spectra of turbulence produced by an ingenious apparatus, employing multiple jets. His results confirm (1.8) and give a form for $F(k/k_s)$.

The fact that laboratory measurements have usually not revealed a significant Kolmogoroff steady-state spectral régime has not, however, lessened interest in this region. It is generally believed that at the much greater Reynolds numbers prevailing in geophysical cases, the régime will be large and important. The experimental confirmation of this expectation is the subject of the present paper.

The value of k_s for the laboratory measurements referred to above is of the same order of magnitude as that found in the work described below. In the laboratory, however, the energy-containing eddies have scales of a few centimetres, while the corresponding scale in the ocean is measured in tens of metres. The greatly increased possibility of statistical de-coupling and local steady state is evident. Expressed in terms of Reynolds number, the channel Reynolds number of the tidal channel 'Seymour Narrows', based upon the depth and the mean velocity, reaches nearly 3×10^8.† This may be compared with Laufer's (1954) pipe, for which the corresponding Reynolds number is 5×10^5. Most of this advantage in Reynolds number results from the greatly increased scale of the motion, although the fact that ν for water is barely one-tenth that for air also contributes.

Reid (1960) has expressed equation (1.5) in a slightly different form. In discussing the Heisenberg theory, he writes

$$E(k) = K_H^{-\frac{3}{2}} \epsilon^{\frac{1}{4}} \nu^{\frac{5}{4}} F(x). \tag{1.10}$$

K_H is a constant and $x = k/k_\eta$, where $k_\eta = (3/8K_H^2 \epsilon \nu^{-3})^{\frac{1}{4}}$. Reid's equation corresponding to (1.8) is

$$\phi(k) = K_H^{-\frac{3}{2}} \epsilon^{\frac{1}{4}} \nu^{\frac{5}{4}} \frac{9}{55} \left(\frac{2^{13}}{3^7}\right)^{\frac{1}{4}} x^{-\frac{5}{3}}. \tag{1.11}$$

Noting that Reid uses a definition of ϕ which is half as large as ours, we have

$$K' = 0{\cdot}302 K_H^{-\frac{3}{2}}.$$

It is thus possible to change the wave-number variable to x in a later section where the experimental observations are compared with theoretical spectra.

It would be remiss not to point out that previous authors have reported measurements of turbulence in natural bodies of water. Bowden & Fairbairn (1956) have reported measurements of both vertical and horizontal turbulent velocities and

† The magnitude of geophysical Reynolds numbers may be appreciated if it is pointed out that a typical interstellar gas cloud 100 light years in diameter, moving at 10 km/sec, has a Reynolds number of only about 10^7.

of the correlation between them, performed with an electromagnetic flowmeter. These authors, however, have not been concerned with the high wave-number part of the spectrum. A group in the U.S.S.R. has used hot-wire methods to measure turbulence in a number of situations (Kolesnikov *et al.* 1958; Kolesnikov 1960). The latter paper describes some measurements of turbulence under ice in the Arctic Ocean in water of uniform density. Estimates of the dissipation rate are given and it is stated (at least in the English translation that is available to us) that Kolmogoroff's law agrees well with the experimental points. The paper, however, is very cryptic and we have not been able to arrive at either of these conclusions on the basis of the data presented. We are therefore not able to compare the results with ours at this time.

2. Experimental equipment

The basic requirements for an instrument to measure small-scale turbulent velocities in sea water are similar to those in air, although numerical specifications can be very different. The velocity sensitive element must have small size, high sensitivity and good high-frequency response. The design problems of instruments for use in air have been widely discussed, and for almost all purposes the hot-wire anemometer is found to have better characteristics than other equipment. The properties of sea water are sufficiently different from those of air, however, that one could not rely entirely on experience in air flows to choose the best principle on which to base an instrument. The obvious properties of sea water which have to be considered are the high density, high drag, the concentration of foreign matter, and the fact that sea water is an electrolyte.

For work under these conditions, propeller-driven current meters become more attractive than they are in air and electromagnetic flowmeters become possible, but the hot-wire type of instrument remains the most promising way of obtaining the required size and frequency response. The first attempts to measure turbulence at this laboratory were with hot wires and the problems of drag and conductivity of the fluid were overcome, but it was found that in most inshore waters the plankton concentration was so high that the wire acquired a heavy coating in a very short time. The sensitivity and frequency response would often fall so rapidly that the wire would be useless in a few minutes. Kolesnikov *et al.* have not reported any trouble with plankton in their work in the Arctic Ocean so there are evidently some places where hot wires can be used.

The instrument to be described uses the same principle as the hot wire but has a probe which is less likely to capture particles than the transverse wire. Figure 1 is a drawing of the probe, which was developed by Ling (1955). The sensitive element is a platinum film about 10^{-6} cm thick which is plated around the tip of a small glass cone. The maximum dimension of the film is less than 0·05 cm. The platinum leads inside the glass tube terminate in a mass of 'platinum sponge' which in turn makes electrical contact with the film.

The probe and bridge originally described by Ling cannot be used in sea water for two reasons. First, because of polarization, the d.c. resistance of the sea-water path decreases with increasing voltage across the probe more rapidly than the resistance of the probe increases. The result is that unless the area of exposed

platinum can be drastically reduced, any d.c. constant-temperature bridge will oscillate. Secondly, the original probe had a resistance of 20 ohms and it cannot be heated by more than about 5° before the current density at the platinum-water interfaces becomes high enough to cause rapid corrosion of the platinum. This latter limitation also applies to a.c. operation, although the details of the corrosion mechanisms are not understood. It has been found necessary to keep the resistance and the area of the film very small so that it can be heated appreciably without applying more than about 1·2 V across it. Although low resistance and small area are desirable, there are practical limits to both these quantities. If the resistance is too small in relation to the resistance of the leads, the sensitivity becomes too low; if the film is too small it becomes too difficult to make. As a result of these considerations, we have developed an a.c. constant-temperature system using 5-ohm probes.

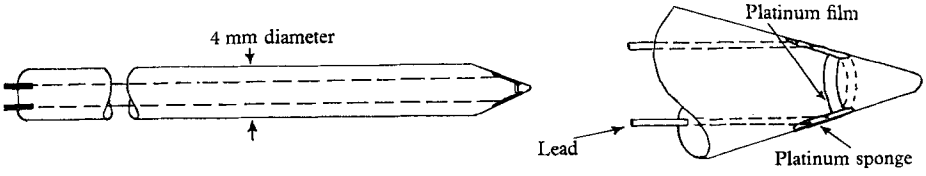

FIGURE 1. The hot-film probe.

A simplified block diagram of the electrical system is given in figure 2. It does not include auxiliary equipment used to measure quantities like depth and inclination of the towed body or calibration and monitoring equipment for the recording. We have also left out the equipment for fast-response temperature measurement which was entangled with that shown here, and used the same tape recorder. There is normally 500 ft. of two-conductor shielded wire between the probe and the ship's laboratory. The transformers near the hot film are used to reflect an impedance of several hundred ohms into the line so that the line impedance is not important. These transformers and the adjacent resistor (which is remotely controlled by a stepping relay) are kept within 30 ft. of the probe. The feedback loop is arranged to keep the bridge as close as possible to balance with varying velocity past the probe. As with a hot wire, the voltage applied to the bridge varies approximately as the fourth root of the velocity. The linearizer is a rectifying and smoothing circuit followed by a tube which operates on the non-linear portion of its characteristics and produces a signal proportional to velocity. Since the gain of the feedback loop is severely limited by unavoidable phase shifts, and the heat loss of the film is not known very accurately as a function of velocity, it would not be safe simply to set the linearizer to produce a fourth power. We therefore calibrate the whole system of bridge and probe in a water tunnel filled with sea water, and set the gain and bias of the linearizer tube so that we obtain an output proportional to velocity with a sensitivity of 0·2 V/cm/sec. The output of the linearizer is displayed on a meter, and, when the flow-meter is in use at sea, this meter reading is continually compared with a similar display from a propeller-driven current meter.

If the linearizer changes slowly with respect to the current meter, the usual cause is a gradual change in water temperature. The remedy is to open the feed-

back loop and turn down the power amplifier, balance the bridge with the film at the new ambient temperature, increase the power amplifier gain until the film is 20° above ambient and close the feedback loop. The last three of these steps are the normal procedure for turning on the equipment. If the linearizer changes suddenly, it means that a plankton particle is caught on the tip of the probe. This happens infrequently in the winter, but in the summer, although most particles bounce off and make only a short spike on the record, one may be caught every 15 min on the average. In February 1960, we could sometimes dislodge dirt

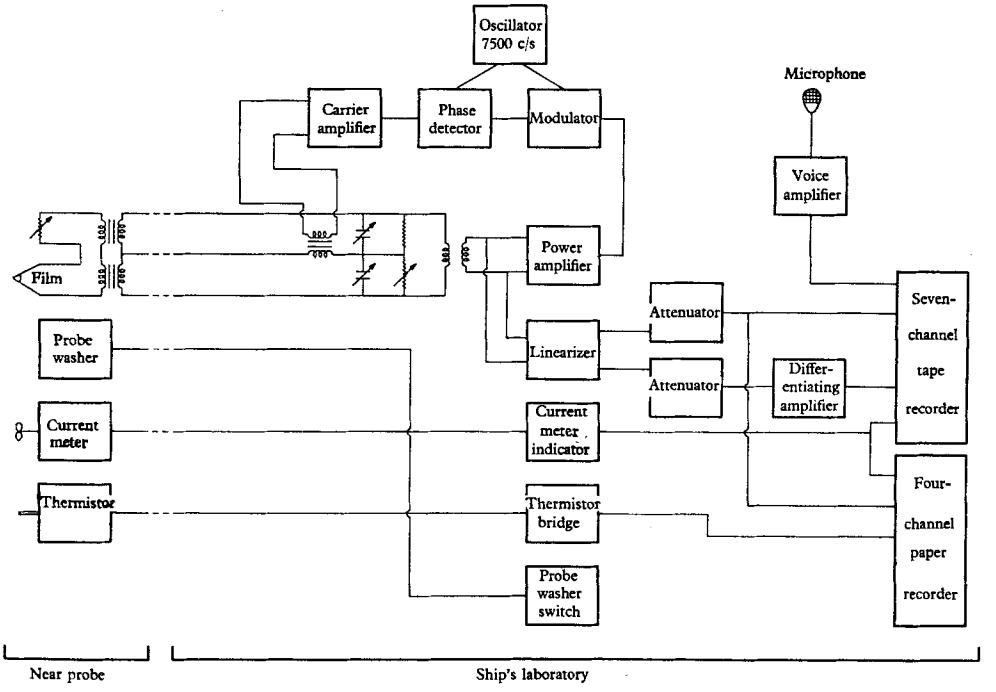

FIGURE 2. Simplified block diagram of the hot film flow-meter and recording equipment.

from the probe by shaking the towing wire, but if this failed, it was necessary to recover the towed body and wash the probe under a tap. Since that time, we have developed a 'probe washer' which disposes of these particles *in situ*.

The output of the linearizer is recorded on magnetic tape, but the spectrum of turbulence falls off so rapidly with frequency that the dynamic range of the tape recorder is insufficient to accept all the information that is available from the flow-meter. For this reason we also record the time derivative of the signal. The spectrum analysis is performed later after return to the laboratory. Other channels of the seven-channel tape recorder are used to record voice (all notes are kept on the tape and transcribed later), current-meter output and temperature.

For observations within 9 ft. of the surface, the hot-film probe is mounted on the bow of the research vessel *Oshawa*. For the measurements to be discussed here, the probe was mounted on a heavy body towed from the quarterdeck as shown in figure 3. This body (figure 4, plate 1), a converted minesweeping

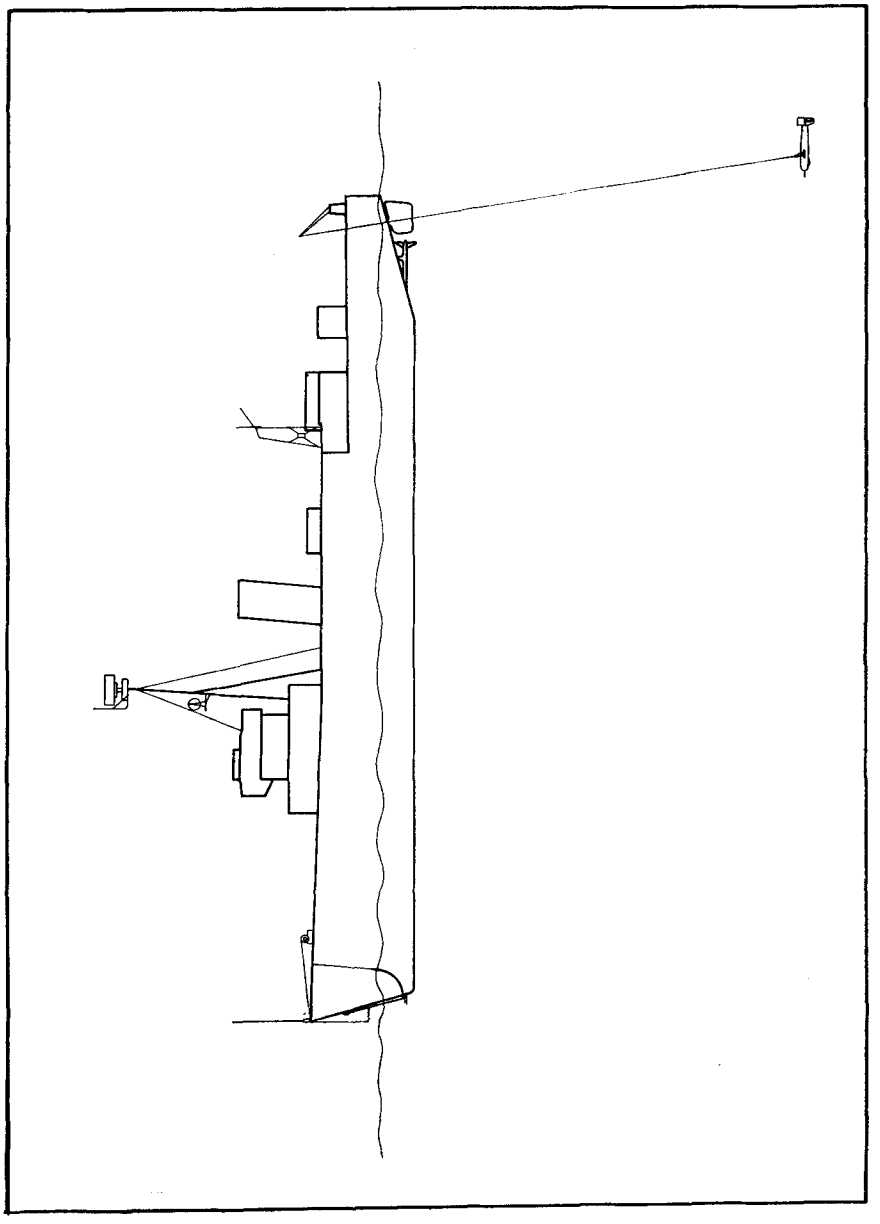

FIGURE 3. The research vessel *Oshawa*, showing the probe mounts on the bow and on the towed body. The overall length of the ship is 217 ft.

paravane, is 12 ft. long and weighs 1500 lb. in air, 300 lb. in water. It can be used at depths between 30 and 200 ft. and was at 50 ft. for these measurements.

Figure 5, plate 2, is a recent picture of the velocity- and temperature-sensing elements mounted on the nose of the towed body. One of the two probes at the left is the hot film and the other is an unheated film used as a fast-response resistance thermometer. This latter instrument was not working properly during the period of observation being discussed in this paper. At the top of the picture is a thermistor and at the bottom a propeller-driven current meter. Each of the probes is mounted in a 'probe washer'. These intricate devices operate on hydraulic pressure of sea water supplied from a pump inside the towed body. When the pressure is applied, by remote control from the ship, the outer barrel of the washer moves forward and sprays the tip of the probe with a high velocity jet. The jet emerges from an annular orifice around the probe and converges at the film with a component of velocity opposite to the normal direction of flow over the film. Before the washers were available, we used probe holders which offered less obstruction to the flow immediately behind the probe, but since the film can now be cleaned in 10 sec instead of 30 or 40 min, the slight change in the mean flow has to be tolerated. The towed body is mostly for calm water use as it pitches violently if the ship rolls, but if the surface is calm, the mechanical noise from vibrations and other motions of the towed body is less than the electronic noise in the high-frequency range. At very low frequencies ($< 0{\cdot}1$ c/s for a towing speed of 125 cm/sec), the ship and towed body may be carried around by the large-scale turbulence with the result that no reliable measurement of turbulent velocity can be made in this frequency range.

The frequency response has been determined by vibrating the probe in a fore-and-aft direction with an electromagnetic driver in a water tunnel. It was found to be flat within 10% from zero to 500 c/s. At frequencies about 500 c/s the vibrator induced several resonant oscillations in the glass probes, and it is not certain that these resonances were not excited by the flow in Discovery Passage. These resonances can be removed by potting most of the glass tube in a brass ferrule, but they were not discovered until after the February cruise, and they might therefore have introduced some error in the spectra at the highest frequencies.

It will be obvious from the character of the spectra that the data are affected by noise at high wave-numbers. If we could measure the noise level independently a correction could be made, but unfortunately this is not easy. We have measured the noise level of the electronics by using a dummy load in place of the probe and we have towed the probe deep in Jervis Inlet where the turbulent energy is very low. On doing this, we get a level which is slightly higher than that produced by the dummy load. This increase in level undoubtedly contains a contribution from the motion of the probe tip arising from vibrations and other movements induced in the towing system by the flow. The dummy load is insensitive to motion, and we have used the 'still water' data rather than the dummy load data for a noise correction. The correction improves the results but is clearly not adequate at the highest frequencies, and the reason may be that the flow-induced motion of the towing system is increased when we work in very violent large-scale turbulence. The correction is insignificant for values of k below 10 cm^{-1} which

corresponds to values of $\log x$ in the vicinity of minus one. Another reason for the inadequacy of the noise correction may have been the presence of some inter-modulation distortion in the power amplifier which is not compensated for by this procedure. The electronic noise level with the dummy load corresponds to an R.M.S. velocity of 10^{-2} cm/sec in the band 1–500 c/s.

Since the hot film is not very hot and is exposed to the sea water, it is sensitive to fluctuations of both temperature and salinity. For a typical probe, these sensitivities are such that a change of 1 °C or 1 ‰ of salinity corresponds to a velocity change of 10 cm/sec. The temperature microstructure is monitored continuously by a thermistor with a frequency response of about 10 c/s, and if the R.M.S. fluctuations exceed 10^{-2} °C the data is considered unreliable. We have not monitored salinity fluctuations but they can be expected to be small in the situations where we have worked.

Figure 6 is a plan of Discovery Passage which is a tidal channel on the west coast of Canada (50° 10′ N., 125° 21′ W.). The current in Seymour Narrows becomes as large as 15 knots and for a 12-knot tide, which is common, the Reynolds number in the Narrows is $2{\cdot}8 \times 10^8$. The present measurements were made between stations two and three where the maximum velocity is about 3 knots. In the latter part of the ebb (north-going) tide, the turbulence is very violent even in this region and it is very difficult for a ship to maintain course at slow speed. We have not kept a detailed record of ship's head but it can be safely said that all the data discussed in this paper were recorded while towing in directions within 20 degrees of the axis of the channel. Depending on the strength of the current, the ship moved either backward or forward with respect to the land, and in the course of an ebb tide we have runs scattered all over this section of the channel.

Although working with geophysical flows gives a large gain in Reynolds number over laboratory experiments, the uncontrollable aspects of the flow obviously introduce some limitations upon the observations. The very size of the flow dictates that we must measure turbulent velocity by means of a probe mounted on a platform which is smaller than most energetic eddies. Although the ship's power can be used to maintain the towing direction reasonably well, there are bound to be large changes in the magnitude of the velocity of the ship and towed body relative to the land.

The longer the homogeneous sample that can be obtained, the more reliable will be spectra derived from it. Our samples have been limited by circumstances beyond our control. We have never succeeded in obtaining a usable homogeneous record of longer than 20 min, and only about 20 % of our total record is in useful stretches of more than 3 min. There are all the usual difficulties of making observations at sea, e.g. that available ship time is limited and scheduled far in advance, with the result that the time for making observations cannot be chosen on the desirable basis of the peak performance of equipment; failures in cables and underwater glands are not unknown; the high humidity and vibration of the ship's laboratory produce difficulties not encountered or expected ashore; the safety of the ship takes precedence over the experiments. An unsuccessful experiment can usually not be repeated before the passage of several months.

We have the advantage, working with a tidal current, of having a predictable steady current with a duration of several hours—but it does not look steady to a 200 ft. ship whose speed is limited to 2·5 knots. Frequently rather violent

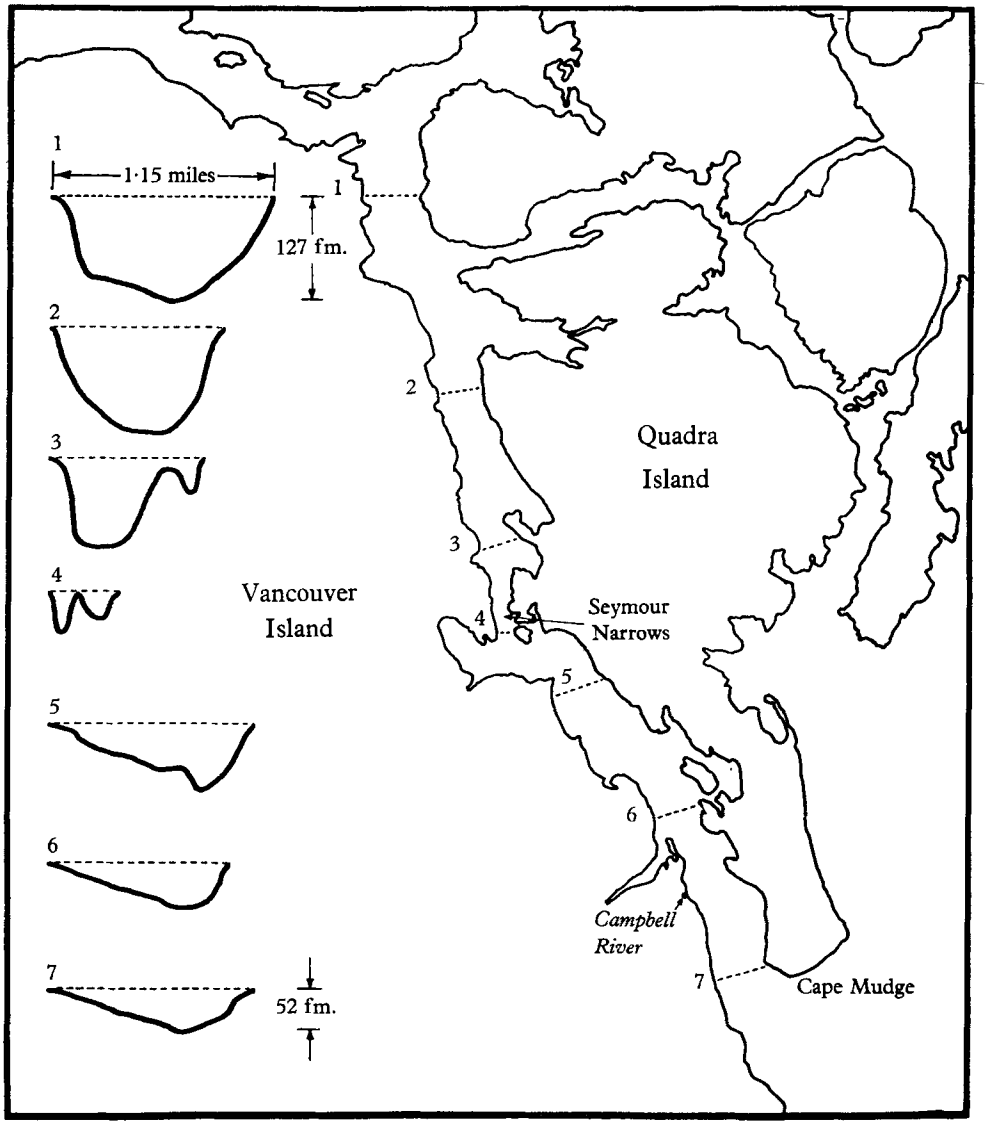

FIGURE 6. Plan of Discovery Passage. (For more detail, refer to the chart listed in the references.)

manoeuvres are required to keep the ship from approaching too close to shallow water. Often we are carried into different regions of the current, where the turbulent intensity is quite different and the record must be interrupted by gain changes. Way has to be made for other shipping, which usually, observing our apparently irrational movements, treats us with some circumspection.

In addition, we may be interrupted by plankton on the probe, by manoeuvres

to avoid the large driftwood (40 ft. logs) common on our coast, or by periods of unacceptably large temperature microstructure.

The reason for using a towing speed of 2·5 knots with respect to the water is that this is the lowest speed at which the ship can be kept under control most of the time. Low speed is desirable because the towed body performs best at low speed and because the smallest scale of motion to which our equipment is sensitive is limited not by the size of the film but by the frequency response of the electronics, and a minimum speed extends our response to maximum values of k.

3. Spectrum analysis

The spectrum analysis of the February 1960 runs has been performed by an analogue circuit which is given in figure 7. Half-octave passive filters were available with centre frequencies 100, 151, 215, 316, 464, 682 and 1000 c/s.

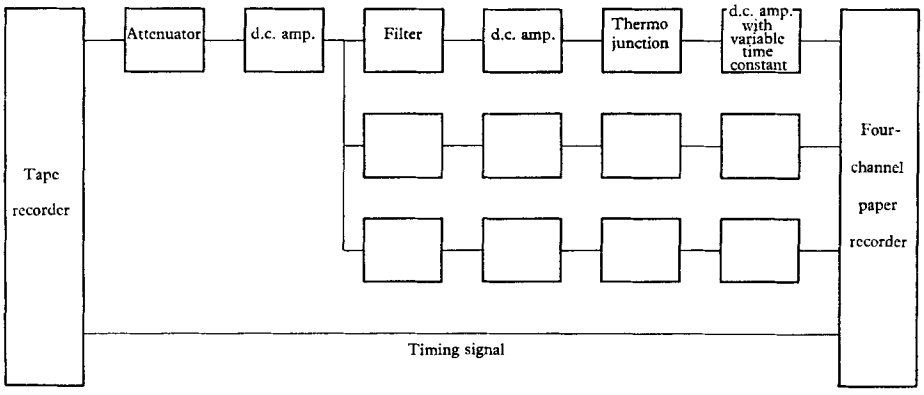

FIGURE 7. Block diagram of the equipment for performing spectrum analyses.

Krohn–Hite variable active filters of about one octave band-width were used for frequencies below 100 c/s. The data were recorded by frequency modulation at a tape speed of 6 in./sec. Each sample was played three times at this speed using different passive filters at each run to cover the range 100–1000 c/s. The tape was then played at 60 in./sec through the same filters to cover the frequency range 10–100 c/s. Points at lower frequencies were obtained with the active filters and a tape speed of 60 in./sec. The time constant of the d.c. amplifier which followed the thermo-junction was made small compared with the time constant of the thermo-junction for the tape speed of 60 in./sec, and ten times the thermo-junction time constant for the tape speed of 6 in./sec. Under these conditions the output of the pen recorder which is the squared and partially averaged signal looks the same for the 100 c/s filter and a tape speed of 6 in./sec as for the 1000 c/s filter and 60 in./sec. The averaging was completed by measuring the area under the trace on the paper record with a planimeter and dividing by the length of the sample. The spectra from the September 1959 runs were obtained in essentially the same way but the variable Krohn–Hite filters were used for all frequencies.

Calibration of the recording and analysis system was obtained by recording a 75 c/s sine wave injected at the plate of the linearizer tube for 5 min every hour during the period of observation. The value of the spectral density is then ob-

tained by an obvious calculation which involves the gains and frequency response of the recording and playback system for the calibration and the signal and also the pre-whitening provided by the differentiating circuits.

It was found that spectral densities obtained with the active filters were higher than those determined with the passive filters. This is apparently due to the effect of the wider pass band operating on the very non-linear spectrum function, so the data obtained with the wide filters have been reduced by an amount averaging 15 % to make it agree with the results from the narrow filters in the overlap region between 10 and 46 c/s.

4. Energy and dissipation spectra

The observations to be discussed were made in October 1959 and February 1960 with the greater part of the data being obtained on the second occasion. The frequency response and high frequency noise level of the equipment were

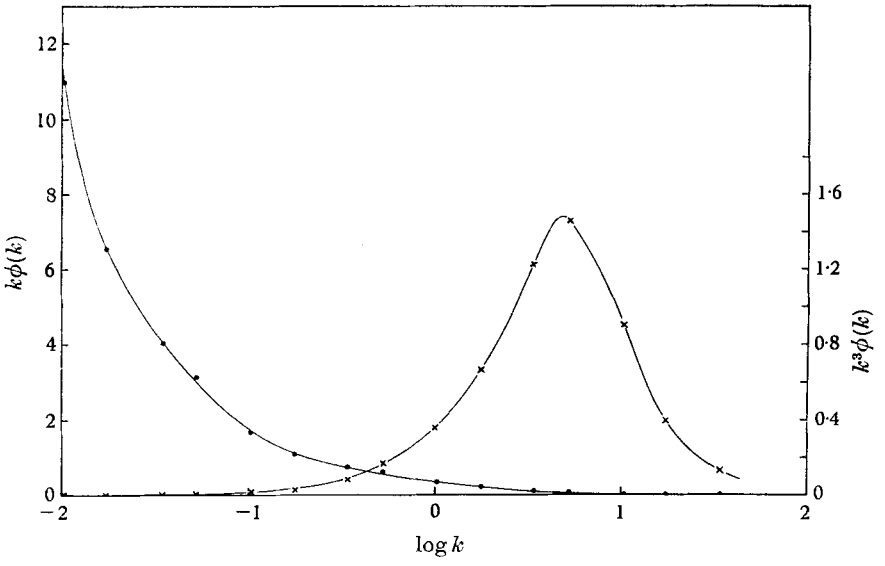

FIGURE 8. Energy and dissipation spectra for the run at 0905/3/10/59. Dots represent the energy spectrum and crosses, the dissipation spectrum.

changed slightly in the interval between the cruises (evidently for the worse), but the sensitivity of the instrument at frequencies below 400 c/s has been maintained to within 10 % for all the data by continuous comparison with the current meter. The greater part of the spectra may therefore be properly compared. It should be noted here that the spectrum obtained in May 1959, published by Grant, Moilliet & Stewart (1959), does not agree well with the present results. Although its shape is satisfactory there appears to have been an error in the calibration.

To illustrate the absolute magnitudes of the quantities involved in a typical run, the spectrum from the 15 min sample at 0905/3/10/59† is plotted in several

† That is 0905 hr, 3 October 1959.

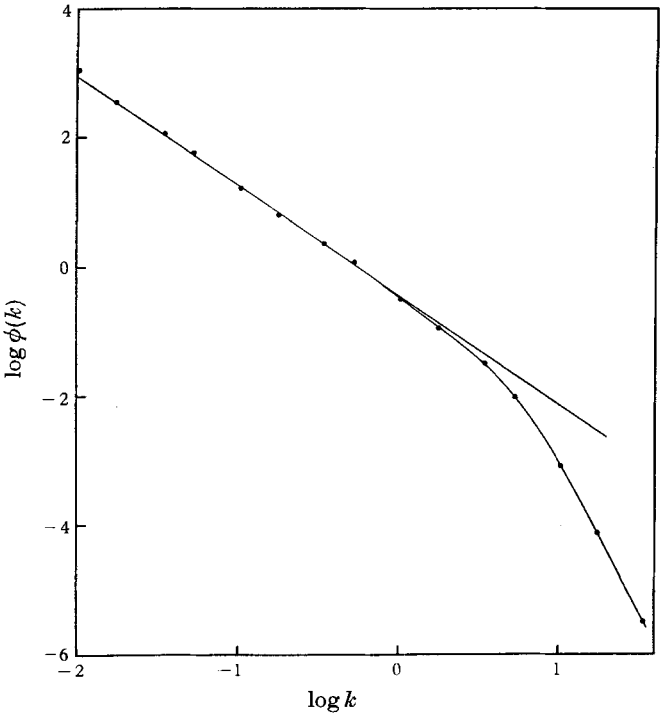

FIGURE 9. A logarithmic plot of the one-dimensional spectrum for the run at 0905/3/10/59. The straight line has a slope of $-\frac{5}{3}$.

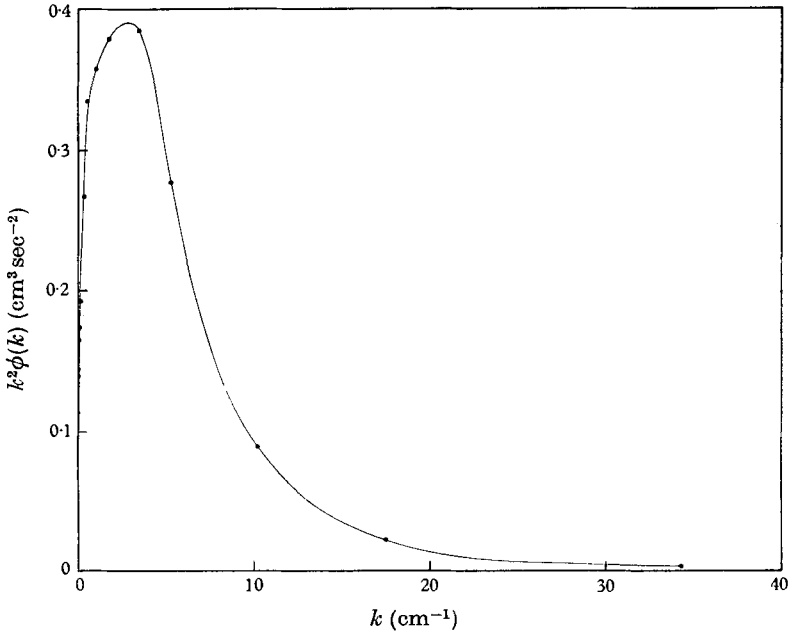

FIGURE 10. Linear plot of the dissipation spectrum for the run at 0905/3/10/59.

ways in figures 8 to 10. The first of these figures shows $k\phi(k)$ and $k^3\phi(k)$ on a linear scale. The spectral densities have been multiplied by k so that the areas under the curves on this semi-logarithmic plot represent the total energy and rate of decay of energy in this part of the spectrum. The left-hand end of the energy curve is obviously incomplete, and this is because, at lower values of k, the scale of the motion approaches the dimensions of the towed body and the ship and so the platform on which the probe is mounted cannot be considered steady. Visual observation of the scale of the surface disturbance in Discovery Passage suggests that the peak of the energy is associated with scales of the order of 50 m.

It can be seen that there is a region of at least one decade on the wave-number scale where the contribution to both spectra is a small part of the total. This is the condition for an inertial subrange, and when the data is presented on a log-log plot (figure 9) we find that this particular spectrum follows very closely the $k^{-\frac{5}{3}}$ law predicted by the Kolmogoroff theory. The fact that the 5/3 law extends over two decades suggests that the area under the curve for k in figure 7 may be negligible compared with the energy in this component of velocity at larger scales. Figure 10 is a linear plot of the dissipation spectrum. It is from graphs like this that the total rate of dissipation has been determined for each run.

It is pointless to show all these runs on individual graphs and several of them are so close together that they cannot be fully presented in one graph. We have therefore provided a numerical table of the results in appendix 1.

Examination of these data will show that the run which has been presented graphically has a smoother dissipation curve than most of the February runs. We believe the reasons for this are that the noise level at the large wave-number end of the spectrum was higher and not so well known in February and that the turbulence level was particularly high during this run.

It is of interest to examine the dependence of the spectra on ϵ, and if we determine ϵ from each dissipation curve and the intercept at $k = 1$ of the best fitting line of slope $-\frac{5}{3}$ on the log-log plot, we can calculate the constant in the Kolmogoroff theory. This has been done for all 17 runs and the result is shown in figure 11. The point at $\epsilon = 0{\cdot}0015$ is derived from a run at a depth of 50 ft. in the open water of Georgia Strait. The turbulence level is very low but the small wave-number end of the spectrum can be represented by a straight line of slope $-\frac{5}{3}$. The dissipation spectrum is disturbed by noise but we know the shape of the spectrum from our other runs, and we have determined ϵ by drawing a spectrum of the proper shape through the lowest points. The value of K' for this run is therefore not as reliable as the others. There might be a slight trend to the values of figure 11 but we are not prepared to say that it is significant without further observation. If we assume that K' is a constant, it is equal to $0{\cdot}47 \pm 0{\cdot}02$ (standard error) for dissipation rates between 0·0015 and 1·02.

Now in order to compare these spectra with the theoretical one-dimensional spectra computed by Reid (1960), we have taken the average value of K' and plotted the results in figures 12 and 13, according to Reid's scaling for the Heisenberg theory. The solid line is the theoretical curve from Heisenberg's theory where the wave-number x is defined in (1.10), and the dashed line from Kovosz-

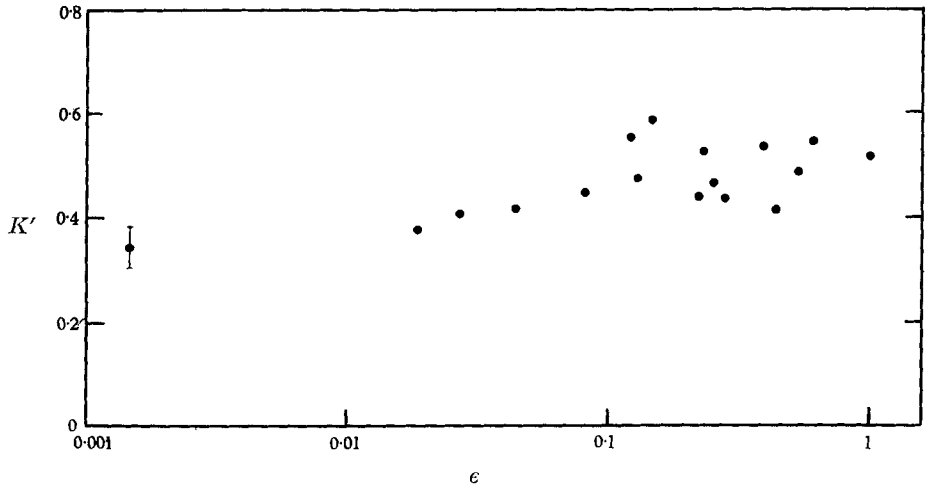

FIGURE 11. Calculated values of the quantity K' as a function of the rate of dissipation of energy.

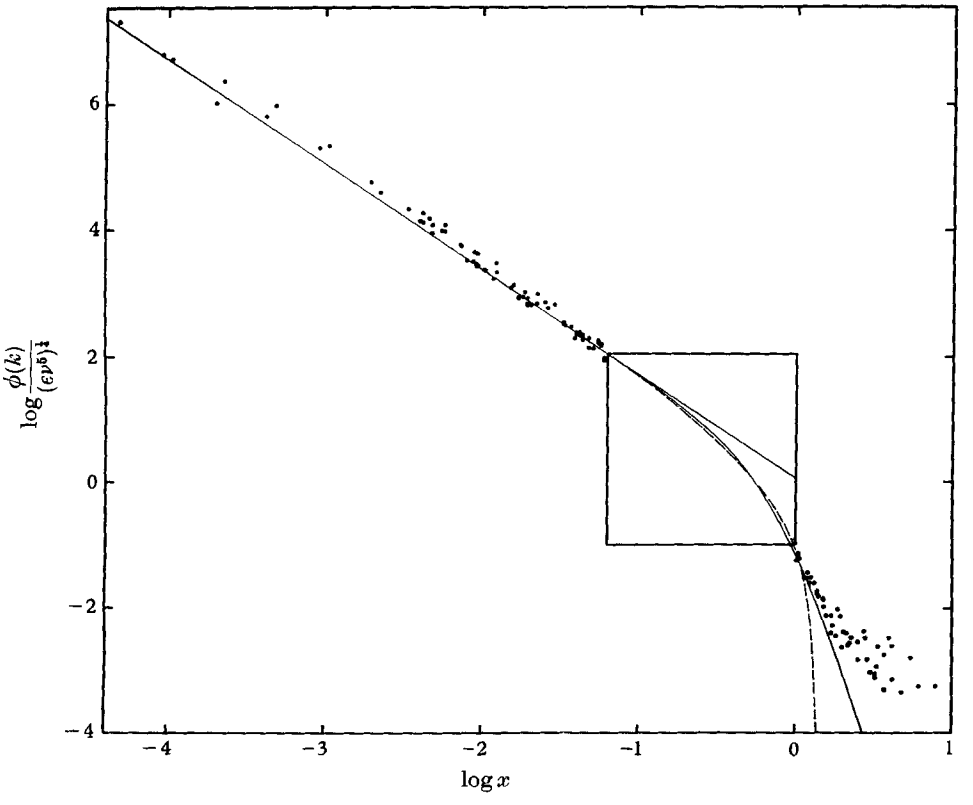

FIGURE 12. Seventeen spectra compared to the theories of Kolmogoroff, Heisenberg and Kovasznay. The straight line has a slope of $-\frac{5}{3}$, the curved solid line is Heisenberg's theory and the dashed line is Kovasznay's theory. Within the square, the observations are too crowded to display on this scale and they are shown in figure 13.

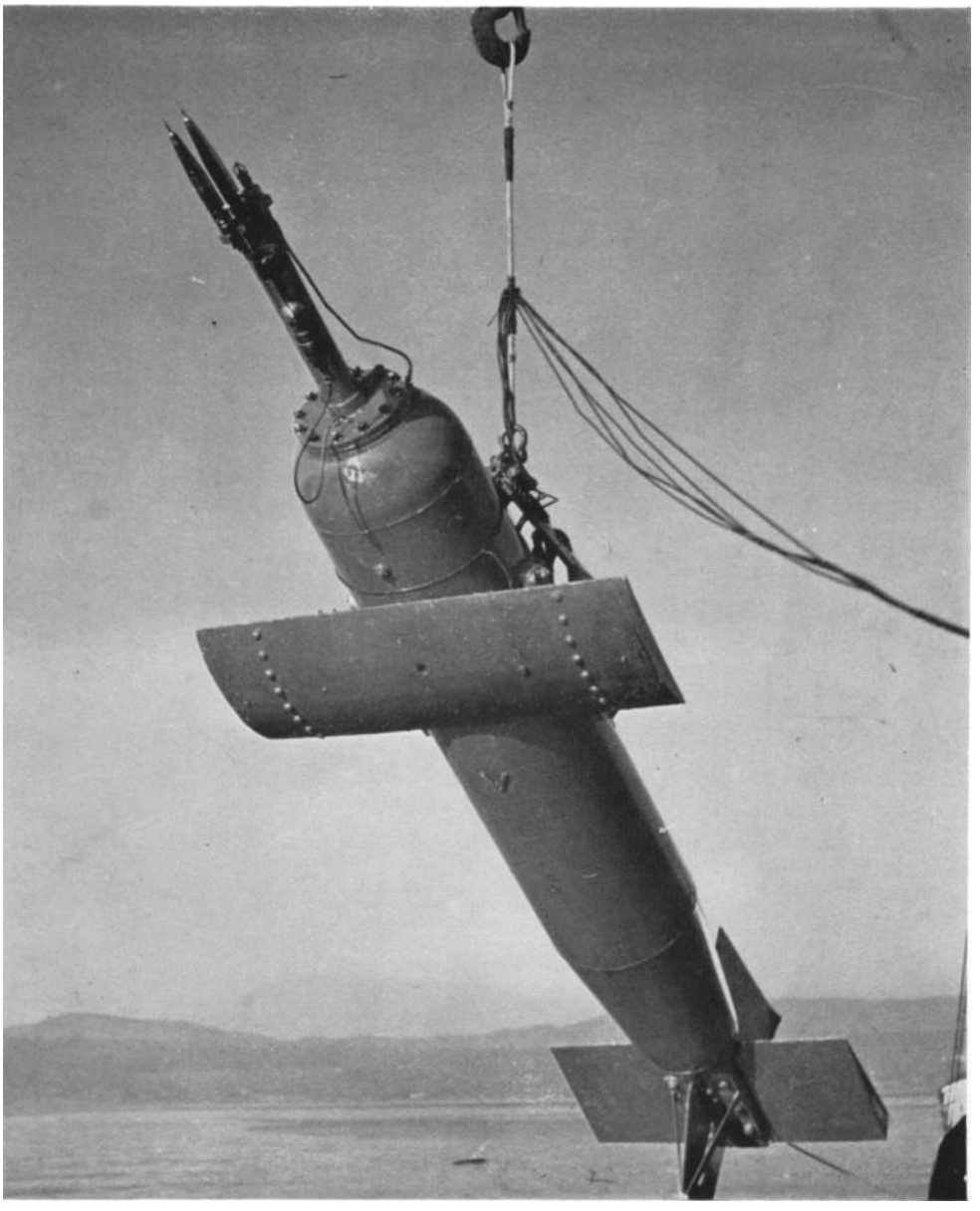

FIGURE 4. The towed body.

FIGURE 5. The nose of the towed body.

nay's.† We have used the following values for the kinematic viscosity: 3 Oct. 1959, $1{\cdot}28 \times 10^{-2}$; 2 Feb. 1960, $1{\cdot}37 \times 10^{-2}$; 3 Feb. 1960, $1{\cdot}42 \times 10^{-2}\,\mathrm{cm^2\,sec^{-1}}$. It is disappointing to see that the two curves diverge sharply just at the point where our data begin to be seriously affected by noise.

At the other end of the spectrum, there is a tendency for points to fall above the line. Since the towed body is only 12 ft. long, we may expect it to be moved about by the large-scale turbulence with resulting errors in the spectrum at low

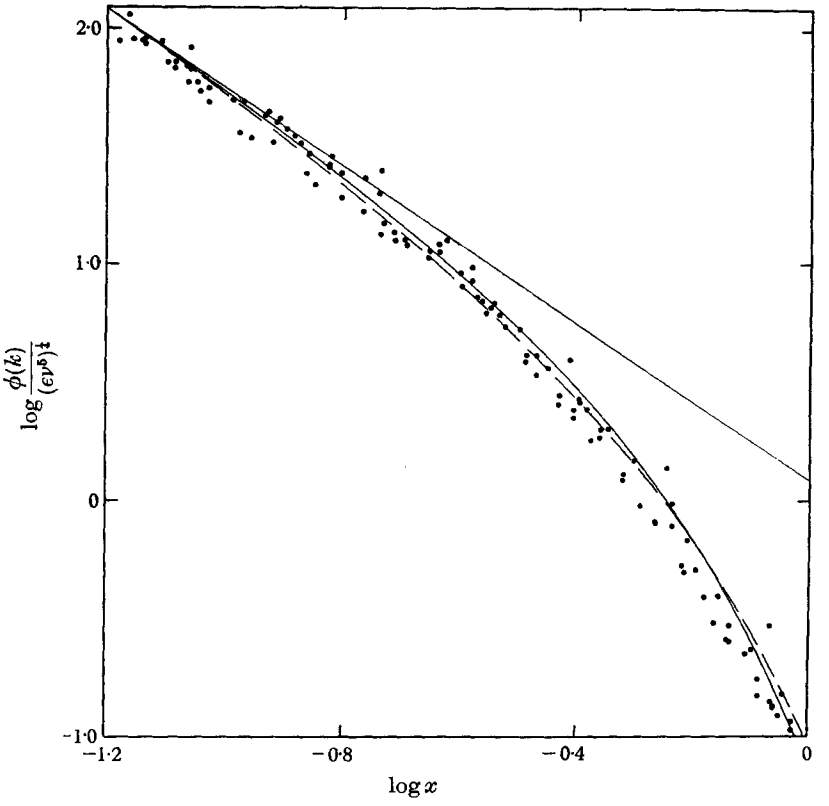

FIGURE 13. The collected spectra in the low wave-number end of the dissipation range.

frequencies. At one time we had a crude accelerometer in the towed body, and it indicated that the motions of the body as a whole were confined to frequencies below 1 c/s. In figure 12, then, we may look for errors from this source for $\log x$ less than approximately $-2{\cdot}2$. The sample length becomes rather short at the extreme end of the curve but these measurements are sufficient to show that even here the spectrum does not deviate much from the $k^{-\frac{5}{3}}$ line.

The points which fall above the line in the region $-2{\cdot}2 < \log x < -1{\cdot}5$ all come from different runs, i.e. no run contributes more than one point, and fewer than half the 17 runs are involved. These runs do not seem to have any peculiar common characteristic and so the displacement of these points from the bulk

† Because of the well known failure of the Obukhov spectrum at high wave-numbers, we have not thought it worth while to compare our results with this theory.

of the data has to be attributed to 'experimental error', but again the motion of the towed body may be the cause.

In figure 14 are a group of ten dissipation curves plotted in a form which allows comparison with the non-dimensional results of Stewart & Townsend (1951)

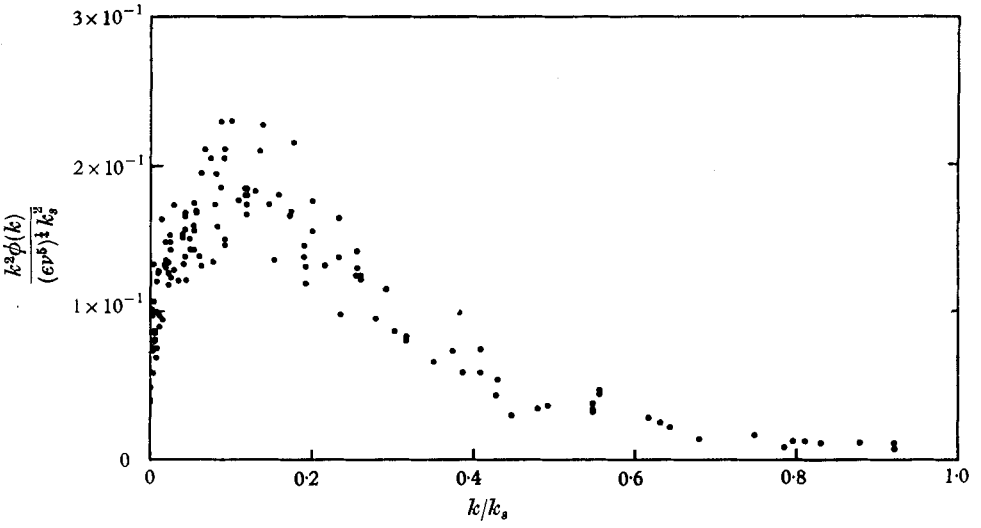

FIGURE 14. Normalized dissipation spectra.

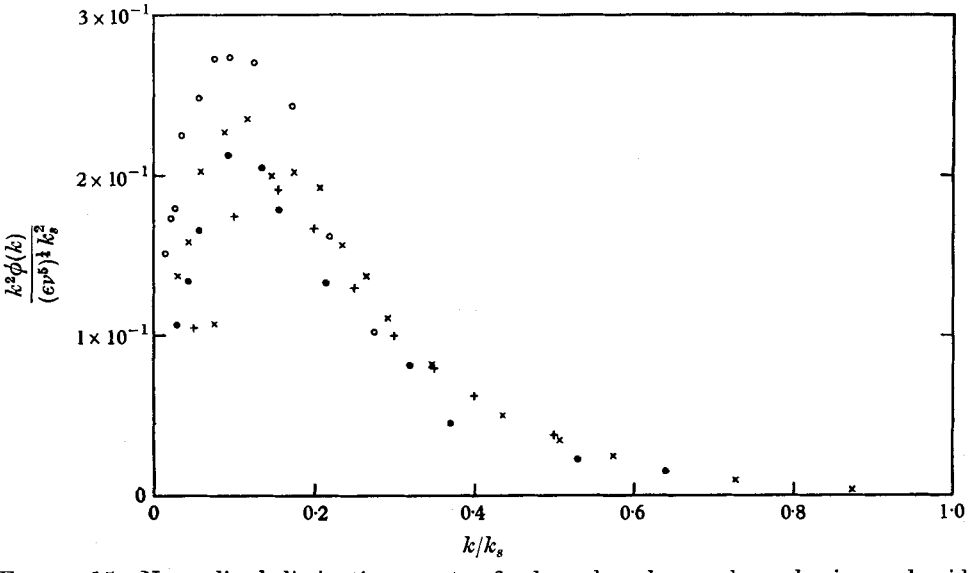

FIGURE 15. Normalized dissipation spectra for boundary layer, channel, pipe and grid turbulence. ×, Channel (Laufer 1951); ○, pipe (Laufer 1954); ●, boundary layer (Klebanoff 1955); +, grid turbulence (Stewart & Townsend 1951, $Rm = 10\,500$).

for grid turbulence. The individual runs are again not identified on the graph, but examination of the data has shown that the scatter is nearly random. This diagram may be compared with figure 15 where we show typical dissipation spectra measured in grid turbulence and in boundary-layer, pipe and channel

flows. In spite of the difference in the Reynolds number, it will be seen that the dissipation spectra in these flows do not differ much in form from those measured in Discovery Passage. Betchov's (1957) results differ so much from those in figures 14 and 15 that they cannot conveniently be plotted on the same scale. His spectrum bends much more sharply than ours at the end of the region of slope $-\frac{5}{3}$, and we are unable to account for this difference.

5. Discussion

The observations reported above give strong support to the Kolmogoroff hypothesis. As is seen in figure 12, all the experimental results can be closely grouped on to one curve if they are made dimensionless by the use of ϵ and ν. Figure 14 shows that the same treatment leaves little difference among observations of high wave-number turbulence by several workers in a variety of turbulent fields.

There is, however, a serious theoretical objection to the concept of a universal high-frequency spectral form which should first be disposed of. This arises from one of the outstanding characteristics of the high wave-number components of measured turbulent fields, intermittency. For example, Batchelor & Townsend (1949) have shown that although the distribution of velocity is closely normal, the distribution of velocity derivatives has a kurtosis considerably greater than 3, even in fully turbulent fields. Close examination of the hot-wire output caused them to conclude that the high kurtosis was due not so much to occasional large values but to occasional regions where the expected value was much larger than in a typical region—in other words, intermittency.

A similar structure has been found by Sandborn (1959) and is very evident in our records. The effect of this intermittency can be seen as random variations in the measured values of ϵ, even though these are evaluated from lengths of record which typically correspond to a distance that is twice the depth of the channel. These values are found to vary by a factor of four or more even when there is no evidence of any change in the overall nature of the turbulence. If ϵ were to be measured from records which were much shorter but still corresponded to a distance very large compared to k_s^{-1}, then the fluctuations in ϵ would undoubtedly be much larger.

Now the basis of the Kolmogoroff hypothesis is the statistical de-coupling of the high wave-numbers from the small wave-numbers, which are closely coupled to the mean flow and must differ appreciably from one turbulent flow to another. According to the hypothesis, of all the information contained in the low wave-numbers only the total dissipation ϵ is not lost in the randomization involved in the transfer of energy to higher and higher wave-numbers. It would seem to be concomitant that if the value of ϵ in one part of the field differs from that in another part of the field, separated by a distance large compared with k_s^{-1}, then the local spectrum should depend upon the local ϵ rather than the value of $\bar{\epsilon}$ obtained by averaging over a much larger spatial region. Precisely how the 'local' value of ϵ should be defined is not immediately clear, but it is evident that there are a number of possibilities which conform to the above discussion.

The idea can be expressed more precisely in spectral terms. $\phi(k)$ is the square

of the modulus of the complex Fourier transform of the velocity component u_i, a function of x_i. When the modulus is taken, phase information is lost. The contention here is that there is a relation among the phases such that if the whole space is divided into regions, each large compared with k_s^{-1}, and a three-dimensional Fourier series decomposition is performed in each region, the modulus of each Fourier component so determined will depend largely upon the dissipation within the region rather than the average dissipation over all regions.

This being the case, then, it becomes evident that one can no longer draw many exact conclusions about measured spectra from the Kolmogoroff hypothesis, for the measured spectra will be averaged over regions with a distribution of values of ϵ. Nothing in the hypothesis, and probably nothing in practice, prevents this distribution from depending upon the mean flow and low wavenumber turbulence. The effect, and its importance, can be illustrated by a greatly simplified example.

Let us suppose that for a region in which ϵ is in some statistical sense uniform, the spectrum is given by

$$\left.\begin{aligned} \phi(k) &= K\epsilon^{\frac{2}{3}}k^{-\frac{5}{3}}, \quad \text{for} \quad k < \left(\frac{\alpha\epsilon}{\nu^3}\right)^{\frac{1}{4}}, \\ &= K\left(\frac{\alpha}{\nu^3}\right)^{\frac{4}{3}}\epsilon^2 k^{-7}, \quad \text{for} \quad k > \left(\frac{\alpha\epsilon}{\nu^3}\right)^{\frac{1}{4}}, \\ \alpha &= \text{const.} \end{aligned}\right\} \tag{5.1}$$

(a spectrum not greatly different from that measured by Betchov 1957).

Let us further suppose that the distribution of ϵ is a simple uniform one given by

$$\left.\begin{aligned} P(\epsilon) &= \frac{1}{(\gamma-1)\epsilon_0} \quad (\epsilon_0 < \epsilon < \gamma\epsilon_0), \\ &= 0 \quad (\epsilon < \epsilon_0,\ \epsilon > \gamma\epsilon_0). \end{aligned}\right\} \tag{5.2}$$

More realistic distributions (Poisson or Gaussian) complicate the mathematics without much improving the demonstration.

In this case the measured value of $\phi(k)$ is

$$\overline{\phi}(k) = \frac{1}{(\gamma-1)\epsilon_0}\int_{\epsilon_0}^{\gamma\epsilon_0}\phi(k)\,d\epsilon, \tag{5.3}$$

and the measured value of ϵ is

$$\bar{\epsilon} = \frac{(\gamma+1)}{2}\epsilon_0. \tag{5.4}$$

$\overline{\phi}(k)$ will now have three ranges: for $k < \left(\frac{\alpha\epsilon_0}{\nu^3}\right)^{\frac{1}{4}}$

$$\overline{\phi}(k) = \frac{3}{5}\frac{(\gamma^{\frac{5}{3}}-1)}{\gamma-1}\left(\frac{2}{\gamma+1}\right)^{\frac{2}{3}}\bar{\epsilon}^{\frac{2}{3}}Kk^{-\frac{5}{3}}, \tag{5.5}$$

for $k > \left(\frac{\alpha\gamma\epsilon_0}{\nu^3}\right)^{\frac{1}{4}}$

$$\overline{\phi}(k) = \frac{1}{3}\frac{(\gamma^3-1)}{\gamma-1}\left(\frac{2}{\gamma+1}\right)^{2}\bar{\epsilon}^2 K\left(\frac{\alpha}{\nu^3}\right)^{\frac{4}{3}}k^{-7}, \tag{5.6}$$

and for intermediate k,

$$\overline{\phi}(k) = \frac{K}{(\gamma+1)\epsilon_0}\left[\tfrac{3}{5}k^{-\frac{5}{3}}\left\{(\gamma\epsilon_0)^{\frac{5}{3}} - \left(\frac{\nu^3k^4}{\alpha}\right)^{\frac{5}{3}}\right\} + \frac{1}{3}\left(\frac{\alpha}{\nu^3}\right)^{\frac{4}{3}}k^{-7}\left\{\left(\frac{\nu^3k^4}{\alpha}\right)^3 - \epsilon_0^3\right\}\right]. \tag{5.7}$$

The not surprising result is that the power laws are unchanged, although the coefficients change, and the transition region is extended in k. The quantitative effect may be illustrated by comparing the results for different values of γ. We have chosen, for illustration, to compare $\gamma = 1$ and $\gamma = 11$.

For $\gamma = 1$, (5.5) yields $\overline{\phi}(k) = \bar{\epsilon}^{\frac{2}{3}} K k^{-\frac{5}{3}}$, while for $\gamma = 11$ we get

$$\overline{\phi}(k) = 0{\cdot}964 \bar{\epsilon}^{\frac{2}{3}} K k^{-\frac{5}{3}}.$$

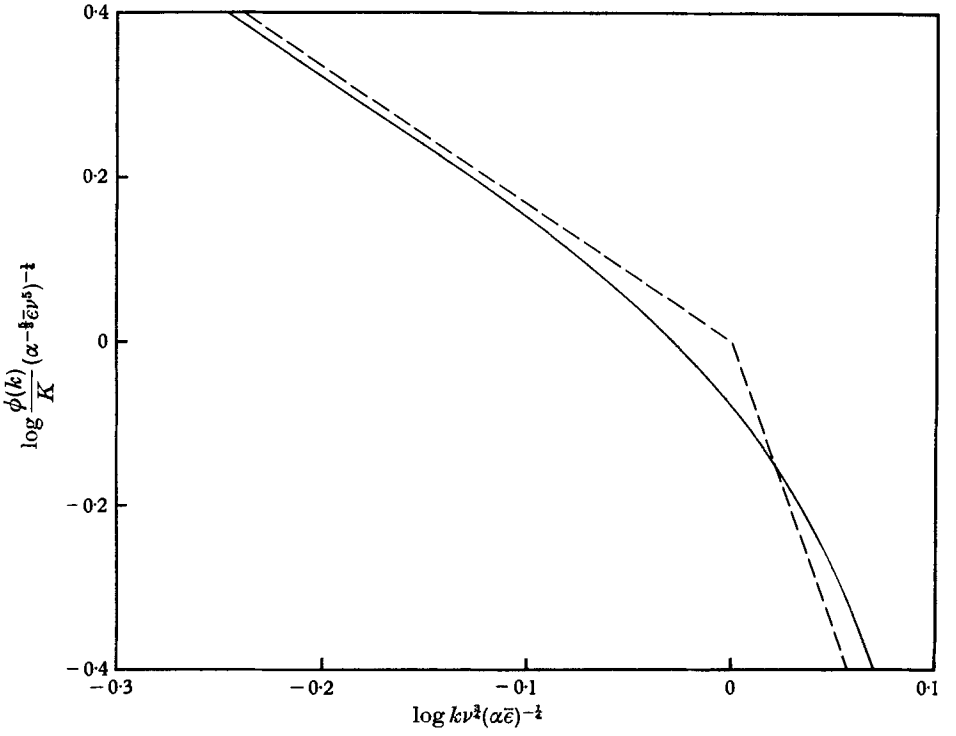

FIGURE 16. The effect on a simple spectrum of a non-uniform spatial distribution of dissipation.

For $\gamma = 1$, (5.6) yields $\overline{\phi}(k) = \bar{\epsilon}^2 K \left(\frac{\alpha}{\nu^3}\right)^{\frac{4}{3}} k^{-7}$, while for $\gamma = 11$ we get

$$\overline{\phi}(k) = 1{\cdot}23 \bar{\epsilon}^2 K \left(\frac{\alpha}{\nu^3}\right)^{\frac{4}{3}} k^{-7}.$$

The difference in the transition region can be seen in figure 16.

A comparison of the scales of figure 16 and figure 12 shows that the effect of a distribution of values of ϵ is in fact of very little importance. It would seem that differences in this distribution can produce only marginal effects on the spectral shapes, and changes in the coefficients of power laws by only a few per cent. Thus while a universal spectrum may not exist exactly, the differences from one field of turbulence to another are negligible unless measurements are available with far greater precision than the present ones.

As yet we have been unable to obtain cross-stream measurements in order to check on high wave-number isotropy. Such measurements are an important part of our future plans, for if further observations confirm the anisotropy reported

by Kistler & Vrebalovich (1961), it is difficult to see how it could be otherwise interpreted than that the Kolmogoroff hypothesis is invalid and the present results are fortuitous.

It is worth noting that our experimental results are reasonably well fitted by both the Heisenberg and the Kovasznay theories. There is some slight tendency for the observations to show less curvature in the transition region than do the theories. This may be related to the distribution of local values of ϵ, as discussed above. The goodness of fit with the Kovasznay theory is worthy of comment. This theory has been largely ignored in comparison with Heisenberg's, but in fact the predictions are closely similar. The Kovasznay form of the transfer function has the great advantage of simplicity. It would appear that it might be used with advantage in coming to grips with such problems as turbulent shear flow.

If we may now accept the Kolmogoroff hypothesis and that we have at least approximate values for K' and for $F(k/k_s)$, several new possibilities are open to us. The most important is that now an observation of a single value of $\phi(k)$ at one value of k will allow us to evaluate ϵ. This means that when working in the presence of noise and vibration we may pick the particular frequency which is least affected by such interference and obtain at least an upper limit for ϵ.

The evaluation of ϵ is probably the most important single measurement in a turbulent field, and important deductions may be made from it alone. For example, if ϵ is measured together with the mean velocity distribution, then the average Reynolds stress may be calculated.

Munk & Macdonald (1960) compute that about $5\,\mathrm{ergs\,cm^{-2}\,sec^{-1}}$ of tidal energy must be dissipated by the ocean. If this dissipation is distributed over the whole ocean we should expect a value of ϵ of about $10^{-5}\,\mathrm{ergs\,cm^{-3}\,sec^{-1}}$ from this cause alone. A dissipation of that magnitude is about 1/150 of the lowest value reported herein. However, a factor of 150 in ϵ yields a factor of less than 30 in $\phi(k)$, and only of about 5 in the signal amplitude. Measurements of such low values of ϵ do not appear out of the question.

Another case, which we expect to deal with in a forthcoming communication, is the dissipation of surface-wave energy by turbulence. In all such cases the measurement of $\phi(k)$ at a single value of k provides us with an upper limit for ϵ and, to the extent that noise can be eliminated or compensated for, an actual evaluation of ϵ.

In developing our equipment, we have received a great deal of assistance from the Engineering Section of the Pacific Naval Laboratory, particularly from Mr H. H. A. Davidson, Mr G. N. Dennison and Mr D. J. Evans. This work would not have been possible without the full co-operation of the crew of the research vessel *Oshawa*. We are especially grateful to Captain Cassidy and to the watch-keeping officers who bore a heavy responsibility not only on the cruises mentioned above but on other occasions when our techniques were under development. Much of the spectrum analysis was performed by Mr C. D. Scarfe with the assistance of Mr R. A. Anderson. Mr R. C. Chappell has made important contributions to the design of the equipment and has been a valued member on all our recent cruises.

REFERENCES

ANONYMOUS 1959 Chart no. 3565, *Discovery Passage*. Canadian Hydrographic Service, Surveys and Mapping Branch, Department of Mines and Technical Surveys, Ottawa.

ANONYMOUS 1959 *Pacific Coast Tide and Current Tables*. Canadian Hydrographic Service.

ANONYMOUS 1960 *Pacific Coast Tide and Current Tables*. Canadian Hydrographic Service.

BATCHELOR, G. K. 1953 *The Theory of Homogeneous Turbulence*. Cambridge University Press.

BATCHELOR, G. K. & TOWNSEND, A. A. 1949 *Proc. Roy. Soc.* A, **199**, 238.

BETCHOV, R. 1957 *J. Fluid Mech.* **3**, 205.

BOWDEN, K. F. & FAIRBAIRN, L. A. 1956 *Proc. Roy. Soc.* A, **237**, 422.

CORRSIN, S. 1958 *N.A.C.A. Research Memorandum*, RM58B11.

GRANT, H. L., MOILLIET, A. & STEWART, R. W. 1959 *Nature, Lond.*, **811**, 808.

HEISENBERG, W. 1948 *Proc. Roy. Soc.* A, **195**, 402.

HINZE, J. O. 1959 *Turbulence*. New York and London: McGraw-Hill Book Co.

KISTLER, A. L. & VREBALOVICH, T. 1961 *Bull. Amer. Phys. Soc.* II, **6**, 207.

KLEBANOFF, P. S. 1955 *N.A.C.A. Report*, no. 1247.

KOLESNIKOV, A. G., PANTELEYEV, N. A., PYRKIN, YU. G., PETROV, V. P. & IVANOV, V. N. 1958 *Isvest. Akad. Nauk SSSR, Ser. Geofiz.* pp. 405–13 (English edition published by American Geophysical Union, July 1959, pp. 229–34).

KOLESNIKOV, A. G. 1960 *Izvest. Akad. Nauk SSSR, Ser. Geofiz.* pp. 1614–23 (English edition published by American Geophysical Union, April 1961, pp. 1079–84).

KOLMOGOROFF, A. N. 1941 *C.R. Acad. Sci., U.R.S.S.* **30**, 301.

KOVASZNAY, L. S. G. 1948 *J. Aero. Soc.* **15**, 745.

LAUFER, J. 1951 *N.A.C.A. Rep.* no. 1053.

LAUFER, J. 1954 *N.A.C.A. Rep.* no. 1174.

LING, S. C. 1955 Ph.D. dissertation, University of Iowa.

MUNK, W. H. & MACDONALD, G. J. F. 1960 *The Rotation of the Earth*. Cambridge University Press.

OBUKHOV, A. M. 1941 *C.R. Acad. Sci., U.R.S.S.* **32**, 19.

REID, W. H. 1960 *Phys. Fluids*, **3**, 72.

SANDBORN, V. A. 1959 *J. Fluid Mech.* **6**, 221.

STEWART, R. W. & TOWNSEND, A. A. 1951 *Phil. Trans.* A, **243**, 359.

Appendix 1. Numerical results

Numerical values of $\phi(k)$ are given in the following tables. U is the mean speed of the towed body relative to the water.

Time of run	0905/3/10/59		0907/3/10/59		0915/3/10/59	
Length of run	15 min		4 min		4 min	
ϵ	0·610 cm² sec⁻³		1·02 cm² sec⁻³		0·395 cm² sec⁻³	
U	117 cm/sec		117 cm/sec		117 cm/sec	
	k	$\phi(k)$	k	$\phi(k)$	k	$\phi(k)$
	34·3	$3·24 \times 10^{-6}$	52·6	$6·90 \times 10^{-7}$	17·5	$3·59 \times 10^{-5}$
	17·5	$7·35 \times 10^{-5}$	34·3	$4·96 \times 10^{-6}$	10·2	$4·58 \times 10^{-4}$
	10·2	$8·59 \times 10^{-4}$	17·5	$1·43 \times 10^{-4}$	5·26	$6·91 \times 10^{-3}$
	5·26	$1·00 \times 10^{-2}$	10·2	$1·67 \times 10^{-3}$	3·43	$2·10 \times 10^{-2}$
	3·43	$3·26 \times 10^{-2}$	5·26	$1·60 \times 10^{-2}$	1·75	$8·81 \times 10^{-2}$
	1·75	$1·24 \times 10^{-1}$	3·43	$5·28 \times 10^{-2}$	1·02	$2·83 \times 10^{-1}$
	1·02	$3·44 \times 10^{-1}$	1·75	$1·92 \times 10^{-1}$	0·526	$9·62 \times 10^{-1}$
	0·526	1·21	1·02	$4·92 \times 10^{-1}$	0·343	1·63
	0·343	2·28	0·526	1·63	0·175	4·95
	0·175	6·32	0·343	3·18		
	0·102	$1·66 \times 10$	0·175	8·52		
	0·0526	$5·96 \times 10$				
	0·0343	$1·18 \times 10^{2}$				
	0·0175	$3·74 \times 10^{2}$				
	0·0102	$1·09 \times 10^{3}$				

Time of run	1126/1/2/60		1203/1/2/60		1304/1/2/60	
Length of run	10 min		8 min		4 min	
ϵ	0·121 cm² sec⁻³		0·235 cm² sec⁻³		0·147 cm² sec⁻¹	
U	127 cm/sec		130 cm/sec		128 cm/sec	
	k	$\phi(k)$	k	$\phi(k)$	k	$\phi(k)$
	33·6	$1·91 \times 10^{-6}$	48·2	$1·50 \times 10^{-6}$	33·4	$1·41 \times 10^{-6}$
	22·9	$3·41 \times 10^{-6}$	32·9	$3·77 \times 10^{-6}$	22·7	$4·46 \times 10^{-6}$
	15·6	$1·18 \times 10^{-5}$	22·4	$9·46 \times 10^{-6}$	15·5	$1·59 \times 10^{-5}$
	10·6	$7·31 \times 10^{-5}$	15·2	$3·57 \times 10^{-5}$	10·5	$8·96 \times 10^{-5}$
	7·45	$3·74 \times 10^{-4}$	10·36	$1·91 \times 10^{-4}$	7·38	$4·36 \times 10^{-4}$
	4·93	$1·95 \times 10^{-3}$	7·27	$8·52 \times 10^{-4}$	4·89	$2·41 \times 10^{-3}$
	4·93	$1·91 \times 10^{-3}$	4·82	$4·28 \times 10^{-3}$	4·89	$2·34 \times 10^{-3}$
	3·36	$6·79 \times 10^{-3}$	4·82	$4·28 \times 10^{-3}$	3·34	$8·22 \times 10^{-3}$
	2·29	$2·06 \times 10^{-2}$	3·29	$1·38 \times 10^{-2}$	2·27	$2·34 \times 10^{-2}$
	1·56	$5·55 \times 10^{-2}$	2·24	$3·74 \times 10^{-2}$	1·55	$6·66 \times 10^{-2}$
	1·06	$1·09 \times 10^{-1}$	1·52	$9·43 \times 10^{-2}$	1·05	$1·16 \times 10^{-1}$
	0·745	$1·87 \times 10^{-1}$	1·04	$1·63 \times 10^{-1}$	0·738	$2·11 \times 10^{-1}$
	0·493	$4·52 \times 10^{-1}$	0·727	$2·92 \times 10^{-1}$	0·489	$5·41 \times 10^{-1}$
	2·29	$2·01 \times 10^{-2}$	0·482	$6·81 \times 10^{-1}$	2·28	$2·29 \times 10^{-2}$
	1·06	$1·15 \times 10^{-1}$	2·24	$3·61 \times 10^{-2}$	1·05	$1·32 \times 10^{-1}$
	0·493	$4·39 \times 10^{-1}$	1·04	$1·73 \times 10^{-1}$	0·489	$5·04 \times 10^{-1}$
	0·229	1·89	0·482	$6·69 \times 10^{-1}$	0·228	2·20
	0·106	6·20	0·224	3·34	0·105	5·18
	0·049	$2·70 \times 10$	0·104	8·00	0·049	$2·87 \times 10$
			0·048	$4·01 \times 10$		

Time of run	...	1319/1/2/60		1331/1/2/60		1216/2/2/60	
Length of run	...	6 min		8 min		4·3 min	
ε	...	0·044 cm² sec^{-1}		0·0187 cm² sec^{-3}		0·441 cm² sec^{-3}	
U	...	129 cm/sec		129 cm/sec		121 cm/sec	
		k	$\phi(k)$	k	$\phi(k)$	k	$\phi(k)$
		22·6	$4{\cdot}70 \times 10^{-6}$	33·2	$9{\cdot}70 \times 10^{-7}$	58·1	$6{\cdot}00 \times 10^{-8}$
		15·9	$7{\cdot}42 \times 10^{-6}$	22·6	$1{\cdot}48 \times 10^{-6}$	35·4	$3{\cdot}74 \times 10^{-6}$
		10·5	$1{\cdot}99 \times 10^{-5}$	15·4	$2{\cdot}67 \times 10^{-6}$	24·0	$1{\cdot}68 \times 10^{-5}$
		7·36	$1{\cdot}22 \times 10^{-4}$	10·45	$7{\cdot}40 \times 10^{-6}$	16·4	$7{\cdot}29 \times 10^{-5}$
		4·88	$5{\cdot}43 \times 10^{-4}$	7·35	$3{\cdot}07 \times 10^{-5}$	11·1	$4{\cdot}05 \times 10^{-4}$
		4·88	$5{\cdot}50 \times 10^{-4}$	4·86	$2{\cdot}45 \times 10^{-4}$	7·82	$1{\cdot}49 \times 10^{-3}$
		3·33	$3{\cdot}17 \times 10^{-3}$	4·86	$2{\cdot}58 \times 10^{-4}$	5·18	$7{\cdot}53 \times 10^{-3}$
		2·26	$7{\cdot}10 \times 10^{-3}$	3·32	$1{\cdot}17 \times 10^{-3}$	5·18	$7{\cdot}87 \times 10^{-3}$
		1·59	$2{\cdot}75 \times 10^{-2}$	2·26	$3{\cdot}14 \times 10^{-3}$	3·54	$2{\cdot}10 \times 10^{-2}$
		1·05	$4{\cdot}03 \times 10^{-2}$	1·54	$1{\cdot}19 \times 10^{-2}$	2·40	$4{\cdot}68 \times 10^{-2}$
		0·736	$7{\cdot}39 \times 10^{-2}$	1·045	$2{\cdot}22 \times 10^{-2}$	1·64	$1{\cdot}13 \times 10^{-1}$
		0·488	$1{\cdot}99 \times 10^{-1}$	0·735	$4{\cdot}19 \times 10^{-2}$	1·11	$1{\cdot}94 \times 10^{-1}$
		2·27	$7{\cdot}79 \times 10^{-3}$	0·486	$9{\cdot}31 \times 10^{-2}$	0·782	$3{\cdot}39 \times 10^{-1}$
		1·05	$4{\cdot}16 \times 10^{-2}$	2·26	$3{\cdot}18 \times 10^{-3}$	0·518	$7{\cdot}16 \times 10^{-1}$
		0·488	$1{\cdot}77 \times 10^{-1}$	1·05	$2{\cdot}17 \times 10^{-2}$	2·41	$4{\cdot}48 \times 10^{-2}$
		0·227	$8{\cdot}79 \times 10^{-1}$	0·486	$9{\cdot}48 \times 10^{-2}$	1·11	$1{\cdot}79 \times 10^{-1}$
		0·105	2·08	0·226	$3{\cdot}83 \times 10^{-1}$	0·518	$8{\cdot}26 \times 10^{-1}$
		0·049	9·46	0·105	1·07	0·241	2·62
		2·27	$7{\cdot}89 \times 10^{-3}$	0·0486	4·82	0·111	$1{\cdot}07 \times 10$
		1·05	$4{\cdot}69 \times 10^{-2}$	2·27	$3{\cdot}90 \times 10^{-3}$	0·052	$5{\cdot}93 \times 10$
		0·488	$1{\cdot}74 \times 10^{-1}$	1·05	$2{\cdot}54 \times 10^{-2}$		
		0·227	$8{\cdot}93 \times 10^{-1}$	0·488	$9{\cdot}09 \times 10^{-2}$		
		0·105	2·52	0·227	$4{\cdot}31 \times 10^{-1}$		
		$k \times 10^3$		0·105	1·24		
		48·8	$1{\cdot}08 \times 10$	$k \times 10^3$			
		22·7	$4{\cdot}67 \times 10$	48·8	5·06		
		10·5	$2{\cdot}55 \times 10^2$	22·7	$2{\cdot}32 \times 10$		
		4·88	$9{\cdot}38 \times 10^2$	10·5	$1{\cdot}04 \times 10^2$		
		2·27	$1{\cdot}56 \times 10^3$	4·88	$3{\cdot}64 \times 10^2$		
		1·05	$3{\cdot}48 \times 10^3$	2·27	$1{\cdot}14 \times 10^3$		
		0·488	$1{\cdot}49 \times 10^4$	1·05	$1{\cdot}84 \times 10^3$		
				0·488	$1{\cdot}10 \times 10^4$		

	1301/2/2/60		1316/2/2/60		1336/2/2/60	
Time of run						
Length of run	15 min		13 min		4 min	
ϵ	0·220 cm² sec⁻³		0·252 cm² sec⁻³		0·537 cm² sec⁻³	
U	132 cm/sec		148 cm/sec		149 cm/sec	
	k	$\phi(k)$	k	$\phi(k)$	k	$\phi(k)$
	32·4	$3{\cdot}84\times10^{-6}$	42·5	$8{\cdot}46\times10^{-6}$	42·1	$1{\cdot}00\times10^{-5}$
	22·0	$1{\cdot}37\times10^{-5}$	29·0	$1{\cdot}14\times10^{-5}$	28·7	$1{\cdot}42\times10^{-5}$
	15·0	$4{\cdot}68\times10^{-5}$	19·8	$2{\cdot}56\times10^{-5}$	19·5	$4{\cdot}99\times10^{-5}$
	10·2	$2{\cdot}22\times10^{-4}$	13·4	$8{\cdot}56\times10^{-5}$	13·3	$2{\cdot}54\times10^{-4}$
	7·17	$9{\cdot}57\times10^{-4}$	9·14	$4{\cdot}09\times10^{-4}$	9·05	$1{\cdot}22\times10^{-3}$
	4·75	$4{\cdot}63\times10^{-3}$	6·25	$1{\cdot}65\times10^{-3}$	6·36	$3{\cdot}83\times10^{-3}$
	4·75	$4{\cdot}24\times10^{-3}$	4·25	$8{\cdot}00\times10^{-3}$	4·21	$1{\cdot}56\times10^{-2}$
	3·24	$1{\cdot}29\times10^{-2}$	4·25	$8{\cdot}40\times10^{-3}$	4·21	$1{\cdot}82\times10^{-2}$
	2·20	$3{\cdot}10\times10^{-2}$	2·90	$2{\cdot}17\times10^{-2}$	2·87	$4{\cdot}55\times10^{-2}$
	1·50	$8{\cdot}05\times10^{-2}$	1·98	$4{\cdot}36\times10^{-2}$	1·95	$9{\cdot}93\times10^{-2}$
	1·02	$1{\cdot}28\times10^{-1}$	1·34	$1{\cdot}17\times10^{-1}$	1·33	$1{\cdot}97\times10^{-1}$
	0·717	$2{\cdot}23\times10^{-1}$	0·914	$1{\cdot}96\times10^{-1}$	0·905	$3{\cdot}67\times10^{-1}$
	0·475	$5{\cdot}22\times10^{-1}$	0·625	$3{\cdot}02\times10^{-1}$	0·636	$5{\cdot}67\times10^{-1}$
	2·21	$3{\cdot}17\times10^{-2}$	0·425	$7{\cdot}92\times10^{-1}$	0·421	1·37
	1·02	$1{\cdot}29\times10^{-1}$	1·98	$4{\cdot}64\times10^{-2}$	1·95	$9{\cdot}63\times10^{-2}$
	0·475	$5{\cdot}09\times10^{-1}$	0·914	$1{\cdot}98\times10^{-1}$	0·905	$3{\cdot}62\times10^{-1}$
	0·221	1·97	0·425	$7{\cdot}42\times10^{-1}$	0·421	1·31
	0·102	9·86	0·198	2·90	0·195	5·66
	0·047	$4{\cdot}01\times10$	0·091	$1{\cdot}53\times10$	0·090	$2{\cdot}35\times10$
			0·042	$6{\cdot}28\times10$	0·042	$8{\cdot}67\times10$

	1340/2/2/60		1440/2/2/60		1445/2/2/60	
Time of run						
Length of run	5·7 min		5 min		6·3 min	
ϵ	0·276 cm² sec⁻³		0·082 cm² sec⁻³		0·131 cm² sec⁻³	
U	149 cm/sec		86·5 cm/sec		103 cm/sec	
	k	$\phi(k)$	k	$\phi(k)$	k	$\phi(k)$
	42·1	$1{\cdot}18\times10^{-5}$	22·9	$1{\cdot}26\times10^{-6}$	28·3	$2{\cdot}24\times10^{-6}$
	28·7	$1{\cdot}47\times10^{-5}$	15·6	$6{\cdot}20\times10^{-6}$	19·3	$7{\cdot}85\times10^{-6}$
	19·5	$3{\cdot}35\times10^{-5}$	11·0	$3{\cdot}94\times10^{-5}$	13·1	$3{\cdot}97\times10^{-5}$
	13·3	$1{\cdot}07\times10^{-4}$	7·26	$2{\cdot}76\times10^{-4}$	9·21	$2{\cdot}13\times10^{-4}$
	9·05	$4{\cdot}82\times10^{-4}$	7·26	$3{\cdot}08\times10^{-4}$	6·10	$1{\cdot}27\times10^{-3}$
	6·30	$1{\cdot}80\times10^{-3}$	4·95	$1{\cdot}28\times10^{-3}$	6·10	$1{\cdot}00\times10^{-3}$
	4·21	$8{\cdot}56\times10^{-3}$	3·37	$4{\cdot}70\times10^{-3}$	4·16	$3{\cdot}49\times10^{-3}$
	4·21	$1{\cdot}03\times10^{-2}$	2·29	$1{\cdot}35\times10^{-2}$	2·83	$1{\cdot}09\times10^{-2}$
	2·87	$2{\cdot}41\times10^{-2}$	1·56	$3{\cdot}15\times10^{-2}$	1·93	$3{\cdot}04\times10^{-2}$
	1·95	$5{\cdot}10\times10^{-2}$	1·10	$5{\cdot}69\times10^{-2}$	1·31	$8{\cdot}36\times10^{-2}$
	1·33	$1{\cdot}28\times10^{-1}$	0·726	$1{\cdot}42\times10^{-1}$	0·921	$1{\cdot}02\times10^{-1}$
	0·905	$1{\cdot}92\times10^{-1}$	3·38	$4{\cdot}68\times10^{-3}$	0·610	$2{\cdot}57\times10^{-1}$
	0·636	$3{\cdot}34\times10^{-1}$	1·56	$3{\cdot}22\times10^{-2}$	2·84	$1{\cdot}14\times10^{-2}$
	0·421	$8{\cdot}33\times10^{-1}$	0·726	$1{\cdot}39\times10^{-1}$	1·31	$6{\cdot}86\times10^{-2}$
	1·95	$5{\cdot}10\times10^{-2}$	0·338	$5{\cdot}68\times10^{-1}$	0·610	$2{\cdot}55\times10^{-1}$
	0·905	$2{\cdot}02\times10^{-1}$	0·156	1·78	0·284	1·03
	0·421	$7{\cdot}92\times10^{-1}$	0·073	$1{\cdot}08\times10$	0·131	3·64
	0·195	3·67			0·061	$1{\cdot}69\times10$
	0·090	$1{\cdot}11\times10$				
	0·042	$4{\cdot}79\times10$				

Time of run	...	1512/2/2/60		1719/3/2/60	
Length of run	...	6 min		8·3 min	
ϵ	...	0·0271 cm^2 sec^{-3}		0·0015 cm^2 sec^{-3}	
U	...	134 cm/sec		121 cm/sec	
		k	$\phi(k)$	k	$\phi(k)$
		46·9	$1·07 \times 10^{-6}$	51·8	$9·24 \times 10^{-6}$
		32·0	$3·12 \times 10^{-6}$	35·4	$5·04 \times 10^{-6}$
		21·8	$3·54 \times 10^{-6}$	23·1	$3·34 \times 10^{-6}$
		14·8	$5·70 \times 10^{-6}$	16·4	$2·53 \times 10^{-6}$
		10·1	$1·50 \times 10^{-5}$	11·1	$5·80 \times 10^{-6}$
		7·08	$7·23 \times 10^{-5}$	7·83	$1·49 \times 10^{-5}$
		4·69	$4·37 \times 10^{-4}$	5·18	$6·59 \times 10^{-5}$
		4·69	$4·63 \times 10^{-4}$	5·18	$5·31 \times 10^{-5}$
		3·20	$1·54 \times 10^{-3}$	3·54	$1·77 \times 10^{-4}$
		2·18	$4·97 \times 10^{-3}$	2·31	$1·70 \times 10^{-4}$
		1·49	$1·76 \times 10^{-2}$	1·64	$1·25 \times 10^{-3}$
		1·01	$3·03 \times 10^{-2}$	1·11	$2·03 \times 10^{-3}$
		0·708	$6·28 \times 10^{-2}$	0·783	$4·55 \times 10^{-3}$
		0·469	$1·41 \times 10^{-1}$	0·518	$1·51 \times 10^{-2}$
		2·18	$4·85 \times 10^{-3}$	2·31	$1·62 \times 10^{-4}$
		1·01	$3·34 \times 10^{-2}$	1·11	$2·34 \times 10^{-3}$
		0·469	$1·32 \times 10^{-1}$	0·518	$1·16 \times 10^{-2}$
		0·218	$5·85 \times 10^{-1}$	0·231	$6·60 \times 10^{-2}$
		0·101	1·71	0·111	$1·80 \times 10^{-1}$
		0·047	6·65	0·052	$8·36 \times 10^{-1}$

Appendix 2. The tidal stream

Day	Time	Speed (knots)	Direction
3 October 1959	0222	11·0	S
	0530	0	
	0831	12·6	N
	1135	0	
	1435	10·7	S
	1738	0	
	2047	13·3	N
	2355	0	
1 February 1960	0145	0	
	0457	10·3	S
	0806	0	
	1121	12·1	N
	1441	0	
	1737	9·2	S
	2047	0	
	2340	9·6	N
2 February 1960	0236	0	
	0544	9·1	S
	0848	0	
	1208	11·2	N
	1530	0	
	1831	8·7	S
	2151	0	

TABLE 1

The predicted tidal currents for Seymour Narrows are given in table 1 (from Pacific Coast Tide and Current Tables, 1959, 1960). Under the heading 'direction', N indicates current flowing from south to north and S the opposite direction.

It is not easy to discover the value of the mean current in the region where we were towing the probe. In table 2, however, we give the position of the ship at intervals of about 30 min and the mean speed through the water as indicated by the current meter (U). The 'speed made good' is the north south component of the ship's movement between fixes and the 'speed of the current' is the difference between the speed relative to the water and the speed made good. The result cannot be very accurate because the current meter was often towed for considerable periods at large angles to the stream.

Under 'ship's head', N and S indicate that the ship is endeavouring to steer a course parallel to the axis of the channel in an approximately northerly or southerly direction. T indicates the position of a 180° turn.

Time and date	Position	U	Speed made good	Speed of current	Ship's head
1205/1/2/60	50° 12′ 11″ N, 125° 22′ 13″ W	—	—	—	S
		2·41 S	1·34 S	1·07 N	
1222/1/2/60	50° 11′ 48″ N, 125° 22′ 29″ W	—	—	—	S
1258/1/2/60	50° 12′ 30″ N, 125° 22′ 12″ W	—	—	—	T
		2·42 N	3·60 N	1·18 N	
1325/1/2/60	50° 14′ 07″ N, 125° 22′ 43″ W	—	—	—	N
		2·53 N	3·48 N	0·95 N	
1345/1/2/60	50° 15′ 17″ N, 125° 23′ 00″ W	—	—	—	T
		2·62 S	17·71 S	0·91 N	
1429/1/2/60	50° 14′ 02″ N, 125° 22′ 42″ W	—	—	—	S
1110/2/2/60	50° 13′ 44″ N, 125° 22′ 58″ W	—	—	—	S
		2·73 S	1·05 S	1·68 N	
1207/2/2/60	50° 12′ 44″ N, 125° 22′ 31″ W	—	—	—	S
		2·53 S	0·71 N	3·24 N	
1232/2/2/60	50° 13′ 02″ N, 125° 22′ 08″ W	—	—	—	T
1243/2/2/60	50° 13′ 26″ N, 125° 22′ 47″ W	—	—	—	T
		2·70 S	0·58 S	2·12 N	
1315/2/2/60	50° 13′ 02″ N, 125° 21′ 54″ W	—	—	—	S
		2·92 S	1·31 S	1·61 N	
1340/2/2/60	50° 12′ 29″ N, 125° 22′ 18″ W	—	—	—	S
		2·76 S	1·55 S	1·21 N	
1408/2/2/60	50° 11′ 45″ N, 125° 22′ 18″ W	—	—	—	S
		2·67 S	0·17 N	2·84 N	
1426/2/2/60	50° 11′ 48″ N, 125° 21′ 45″ W	—	—	—	S
		2·51 S	1·34 N	3·85 N	
1506/2/2/60	50° 12′ 42″ N, 125° 22′ 24″ W	—	—	—	S
		2·55 S	1·00 S	1·55 N	
1530/2/2/60	50° 12′ 18″ N, 125° 22′ 34″ W	—	—	—	S

TABLE 2